Journal of Particle Science and Technology 11 (1) (2025) 1-10

Iranian Research Organization for Science and Technology (IROST)

Journal of PARTICLE Science & Technology

JPSIT
https://jpst.irost.ir

Online ISSN: 2423-4079
Print ISSN: 2423-4087

Effects of hybrid confinement potential on predictable hadronic highly resonance states

Arezu Jahanshir[1,✉], **Ekwevugb Omugbe**[2]

[1] *Department of Physics and Engineering Sciences, Buein Zahra Technical University, Qazvin, Iran*
[2] *Department of Physics, University of Agriculture and Environmental Sciences Umuagwo, Imo State, Nigeria*

HIGHLIGHTS

- Mass spectra of highly excited states of Bottomia are calculated.
- Relativistic correction on mass is defined.
- Relativistic correction effect on the shape of the hybrid potential is plotted.

GRAPHICAL ABSTRACT

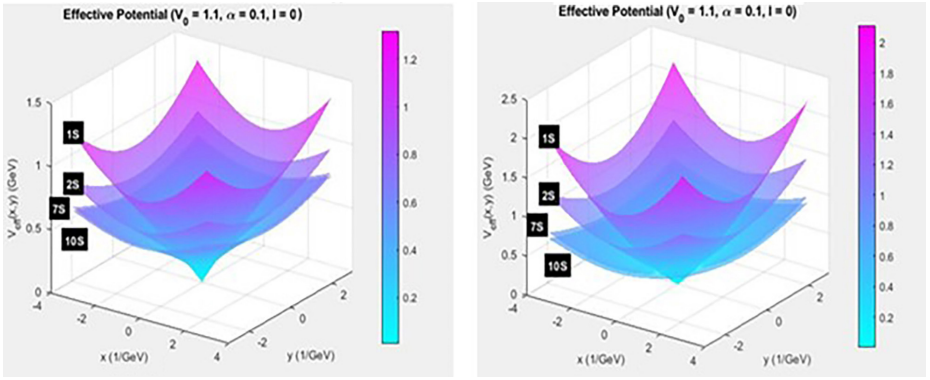

ARTICLE INFO

Article type:

Research article

Article history:

Received 11 May 2025
Received in revised form 11 June 2025
Accepted 25 June 2025

Keywords:

Highly excited states
Hybrid potential
Relativistic correction
Variational method

ABSTRACT

Unlike light quarkonium bound states, the relativistic effects in highly massive quarkonium states, such as Bottomia, in the large radial excitation states, cause Bottomia to have a strong reaction and sensitivity to relativistic corrections. Highly excited states have a larger separation distance between the constituent quark-antiquark pair in the bound state. Therefore, they will have a relatively high velocity, which makes the relativistic kinetic energy and relativistic mass of quarks non-negligible. Notably, in this study, one of the important behaviors of relativistic effects of predicted highly excited hadronic bound states of Bottomia within the hybrid confinement potential is obtained. The high-energy refinement and relativistic effect modification of mass and kinematic energy are defined within the formalism of quantum oscillator principles and quantum field theory, utilizing the auxiliary variational method. Relativistic corrections and effects on the shape of the potential due to relativistic mass are plotted and compared to the calculated non-relativistic plots. The values of the mass spectra of Bottomia used in the potential plot are consistent with predictions from other theoretical approaches and explain the behavior of the results obtained by the used method.

DOI: 10.22104/jpst.2025.7612.1277

✉ *Corresponding author: E-mail address:* jahanshir@bzte.ac.ir ; *Tel:* +98283-3894000

1. Introduction

The different spin arrangement properties of angular momentum states in predicted highly excited Bottomia bound states ($b-b^*$), among other highly resonance states, are important and significant [1,2]. These highly massive resonance states have been distinguished based on the theoretical behaviors of the standard quark model, allowing us to explore various phenomena associated with bound states. The hybrid confinement potential (HCP) model in quantum chromodynamics (QCD) plays an important role in reviewing and analyzing the characteristics of strongly excited resonance states of Bottomia. These types of potentials help us understand the perturbative and nonperturbative Hamiltonian of interactions, particle dynamics, decay rates, bound state properties, and quark-gluon dynamics in high-energy physics and ultra-hot media. In the last experimental research from the LHC, Super KEKB accelerator (Belle II), ALICE Experiment, LHCb Experiment, CMS and ATLAS Experiments, the highly resonant states of Bottomia, such as $7s:\Upsilon(10860)$ and $10s:\Upsilon(11020)$, can be better described and analyzed using the HCP model [3,4]. The calculated spectra of Bottomia, based on Coulombic and confinement characteristics of potential models, closely align with experimental results obtained from strong interaction. The mass spectroscopy of bound states, decay channels, transition rates, hybrid states, relativistic corrections to mass, nonperturbative potentials, wavefunction analysis, and decay mechanisms under extreme ultra-hot temperature conditions in high-energy physics can be investigated more effectively within HCP models. Hence, predicting new resonance states of Bottomia and new exotic hadronic bound states is enabled by determining mass spectra under a specific potential model.

This intertwined space of experimental and theoretical knowledge regarding additional excitations and more complex hadronic states is filled and completed by studying the properties of Bottomia-bound states. Bottomia, based on its relativistic and nonperturbative properties, is the best candidate for investigating hybrid states because most of the expected behaviors of its resonance states exhibit certain anomalies [5]. These anomalies can describe potential impact factors and transition rates. As we know, recent research and studies have focused on the relativistic behaviors of Bottomia in highly excited states, leading to improved theoretical calculations of mass spectra using relativistic mass. Hence, in this article, we define relativistic corrections on mass and potential interaction in Bottomia bound states. The paper is organized as follows: In section 2, we determine the mass and constituent mass of Bottomia bound states, based on canonical variable transformations in symplectic space under the oscillator representation method, where the wavefunction is presented as a Gaussian basis function. In section 3, the relativistic radial Schrödinger equation (RRSE) is solved using relativistic energy within the HCP framework. In section 4, we plot the effective potential shape under various effective potential parameters, i.e., μ_b , ξ with the non-relativistic and relativistic RSE, defining relativistic corrections on mass spectra and eigenenergies of excited states. In the last section, the practical application of the results of theoretical calculations of the mass spectrum and interaction potential behavior is demonstrated. We used computational coding and graph visualization with *MATLAB R2021a* software, and for additional mass spectra calculations, we employed Excel 2022 software.

2. Relativistic form of the Schrödinger equation

We have defined the bound state properties using quantum field theory and the Feynman path integral method within the formalism of a gauge boson interaction with $b-b^*$ pairs, based on the theoretical definition of the vacuum polarization corrections that connect different loop diagrams in Feynman path integrals [6-8]. The non-relativistic and relativistic radial Schrödinger equation reads:

$$H\Psi(r) = E(\mu)\Psi(r) \tag{1}$$

$$H_{rel}\Psi(r) = E(\mu)\Psi(r) \tag{2}$$

Therefore, for $b-b^*$pairs the bound state takes the form of non-RRSE

$$\left(\frac{\hat{p}_r^2}{2m_b^2} + \frac{\hat{p}_r^2}{2m_{b^*}^2} + V(r)\right)\Psi(r) = E(m_b, m_{b^*})\Psi(r) \tag{3}$$

This formula can be easily solved by many different methods. For example, by modifying Eq. (1), one has the RRSE model in the following form,

$$H_{rel}\Psi(r) = E(\mu)\Psi(r)$$

which can be defined by changing classical kinetic energy to the total relativistic energy as follows:

$$\frac{1}{2}m_0v^2 \to \sqrt{m_0^2 + p_r^2}$$

where m_0 is the rest mass and p_r is the relative radial momentum of a quark-antiquark pair in a bound state. On the other hand, as we know, the inequality of the arithmetic and geometric inequality equation in mathematics holds for two non-negative numbers x and y with equality if and only if $x = y$, as follows.

$$\frac{x+y}{2} \geqslant \sqrt{xy}$$

Choosing $x = \mu$ and $y = \frac{m_0^2+\hat{p}_r^2}{\mu}$, then

$$f(\mu^*) \geqslant \sqrt{\mu^* \cdot \frac{m_0^2+\hat{p}_r^2}{\mu^*}} = \sqrt{m_0^2+\hat{p}_r^2}$$

One considers that the arithmetic mean of a set of non-negative real numbers is greater than or equal to the geometric mean of the same set. The minimal (optimal) choice of parameter μ^* is defined when $\mu^* = \frac{m_0^2+\hat{p}_r^2}{\mu^*}$; therefore, we have

$$\mu^{*2} = m_0^2+\hat{p}_r^2 \rightarrow \mu^* = \sqrt{m_0^2+\hat{p}_r^2}$$

and one can define the minimum value of the function $f(\mu)$ within the minimal choice of $\mu^* = \mu$, which is equal to

$$\min_{\mu>0} f(\mu) = \sqrt{m_0^2+\hat{p}_r^2}$$

Inserting the minimal value μ back into the first relationship gives us

$$\sqrt{m_0^2+\hat{p}_r^2} = \frac{1}{2}\left(\sqrt{m_0^2+\hat{p}_r^2} + \frac{m_0^2+\hat{p}_r^2}{\sqrt{m_0^2+\hat{p}_r^2}}\right)$$

Using this equation, we define the effective mass approximation in high energy physics in the form of

$$\sqrt{m_0^2+\hat{p}_r^2} = \min_{\mu>0}\frac{1}{2}\left(\mu + \frac{m_0^2+\hat{p}_r^2}{\mu}\right)$$

where the minimal value choice of this parameter μ is given for the mass of the particle. Below, we consider this optimal value as the relativistic mass of a particle in bound states or the constituent mass of particles in the context of high energy physics. Now, we use a mass approximation in Eq. (2) for the bound states of the pair $b-b^*$ within the potential of interaction $V(r)$ with the rest masses $m_b = m_{b^*} = m_0$ and the relative momentum $|\hat{p}_{rb}^2| = |\hat{p}_{rb^*}^2| = |\hat{p}_r^2|$ as follows:

$$\left(2\min_{\mu_b}\frac{1}{2}\left(\mu_b + \frac{m_0^2+\hat{p}_r^2}{\mu_b}\right) + V(r)\right)\Psi(r) = E(\mu_b)\Psi(r) \quad (4)$$

where parameter $\mu_b = \mu_{b^*}$ is the relativistic mass correction of the rest mass of the pair $b-b^*$ in the bound states (constituent mass of particles). To describe two-particle interactions and neglect the spin interactions, we use the principles of quantum mechanics (QM) and quantum field theory (QFT). As we know, the probability amplitude for a particle's (the pair $b-b^*$) transformation from x_b, x_{b^*} to y_b, y_{b^*} under the external quantum gauge field A_α is described by the propagator function [7,8]. The initial and final states of $b-b^*$ bound states are connected by this function and determine how the bottom and antibottom quarks travel over spacetime in the Minkowski coordinate system. In QM and QFT, Green's function [9] is presented as a propagator in the form of

$$G(x_b, x_{b^*}; y_b, y_{b^*} \mid A_\alpha) = \langle y_b, y_{b^*}|e^{-iHt}|x_b, x_{b^*}\rangle$$

and the interaction of the pair $b-b^*$ is described by $\Pi(x_b, x_{b^*}; y_b, y_{b^*})$ polarization loop operator

$$\Pi(x_b, x_{b^*}; y_b, y_{b^*}) = \langle G_b(x_b, x_{b^*}; y_b, y_{b^*}|A_\alpha)G_{b^*}(x_b, x_{b^*}; y_b, y_{b^*} \mid A_\alpha)\rangle_{A_\alpha}$$

and the field propagator by Green's function

$$\delta^{(4)}(x_b, x_{b^*})\delta^{(4)}(y_b, y_{b^*}) = \left[\left(i\gamma_b^\alpha \partial_{\alpha,b} + igA_\alpha\right) - m_b^2\right]G(x_b, x_{b^*}; y_b, y_{b^*} \mid A_\alpha) + \left[\left(i\gamma_{b^*}^\alpha \partial_{\alpha,b^*} + igA_\alpha\right) - m_{b^*}^2\right]G(x_b, x_{b^*;}, y_b, y_{b^*} \mid A_\alpha) + V(x_b, x_{b^*}; y_b, y_{b^*}|x_b, x_{b^*}; y_b, y_{b^*}) \quad (5)$$

Eq. (3) describes an effective interaction of two particles for creating the bound states in an external field within a potential interaction in QFT [9,10]. We have to average and integrate over the external field to determine properties and all possible configurations of interaction using Eq. (3). This equation explains the external field reaction to a disturbance of the bounded particles at y_b, y_{b^*}. Based on the context of quantum chromodynamics (QCD) in high energy limits, we consider the long-range forces $\left((x_b, x_{b^*}) - (y_b, y_{b^*})\right)$ that lead to creating a Bottomia bound state with the mass M, and rewrite the behavior of the polarization loop operator in the form [11,12].

$$\Pi(x_b, x_{b^*}; y_b, y_{b^*}) = \int \frac{d^4}{(2\pi)^4}\frac{1}{p^2-M^2+i\varepsilon}e^{ip(x_b,x_{b^*};y_b,y_{b^*})} \quad (6)$$

As the pair $b-b^*$ loop function $\Pi(x_b, x_{b^*}; y_b, y_{b^*})$ decays exponentially, this gives us a functional equation to calculate the mass spectra

$$\Pi(x_b, x_{b^*}; y_b, y_{b^*}) = C.e^{-M|(x_b,x_{b^*})-(y_b,y_{b^*})|}$$

where C is a normalization constant. Its value can be determined from the properties of the wavefunction of the bound state, the boundary conditions of the bound state, and

the interaction kernel. The specific conditions $M < \infty$ and $M = m_b + m_{b^*}$ are necessary to create a bound state. Next, the polarization loop operator using QM principles based on the Feynman path-integral formulation [6-8], was used to to determine the two-point correlationfunctions of fields with the rest masses m_b, m_{b^*} as follows,

$$\Pi(x|A) = \int_0^\infty \int_0^\infty \frac{d\mu_b d\mu_{b^*}}{(8x\pi^2)^2} I(\mu_b, \mu_{b^*}) e^{-\frac{|x|}{2}\left[\left(\frac{m_b^2}{\mu_b}+\mu_b\right)+\left(\frac{m_{b^*}^2}{\mu_{b^*}}+\mu_{b^*}\right)\right]}$$

where $x = (x_b, x_{b^*}) - (y_b, y_{b^*})$, parameter μ_b, μ_{b^*} are the constituent masses of particles in the bound states. These masses are presented as the relativistic mass of particles based on Eq. (2). After some mathematical corrections, the mass spectrum of the bound state is defined as

$$M = \lim_{|x|\to\infty)} \frac{-ln\, \Pi(x)}{|x|}$$

and after some mathematical adjustments and using the saddle point method from Eq. (2), the mass spectrum of the pair $b - b^*$ bound state based on the rest mass $m_b = m_{b^*}$, the constituent mass $\mu_b = \mu_{b^*}$, and $E(\mu_b)$ energy of bound states reads as [13,14].

$$M = \min_{\mu_b}\left(\frac{m_b^2}{\mu_b} + \mu_b + E(\mu_b)\right) \quad (7)$$

To minimize this equation, we define the constituent mass equation of the quark as follows.

$$\mu_b = \sqrt{m_b^2 - \mu_b^2 \frac{dE(\mu_b)}{d\mu_b}} \quad (8)$$

Hence, the interaction of the pair $b - b^*$ containing potential and nonpotential terms is modified under the Feynman path integral (functional integral) in non-relativistic theory and reads as

$$I(\mu_b) = C^* e^{-x\, E(\mu_b)}$$

where C^* is a constant and depends on the normalization and boundary conditions of the bound state.

3. Relativistic correction on the interaction potential

In this section, we present the relativistic mass correction and effects on the energy eigenvalue within HCP of $7s{:}\,\Upsilon(10860)$ and $10s{:}\,\Upsilon(11020)$. Starting from Eq. (2) and solving RRSE under the Gaussian basis function method (GBM) for $b - b^*$ bound states within the HCP of the form

$$V(r) = -V_0 \frac{e^{\alpha r} - e^{-\alpha r}}{e^{\alpha r} + e^{-\alpha r}} + \sigma r$$

where $V_0 \succ 0$ α, and σ are constant with the specific values that are adjusted to match the experimental data of highly states of Bottomia [15]. HCP is important in high energy physics because of the complex interplay between two specific forces at short and long distances in QM, QFT, spectroscopy, and quark-antiquark interactions. Choosing HCP in hyperbolic $tanh(ar)$ or exponential forms with the confinement term, we can explain the balance between short and long interaction range [16]. The radial excitation and orbital excitation based on the physical structure of the quarkonium system can better describe theoretical predictions and experimental data under this type of potential. Using GBM or effective field models, HCP can refine spectral interpretation states [17]. This potential allows us to include a discussion on nonperturbative effects in strong coupling interactions in hadronic states and analyze the behaviors of $b - b^*$ bound states under different kinds of interactions. GBM allows us to define and determine relativistic effects of a bound state problem in QCD and hadronic spectroscopy in high energy physics by setting the pair $b - b^*$ as a quantum harmonic oscillator bound state. GBM helps us to represent canonical variables $\hat{x} = \frac{(\hat{a}^+ + \hat{a})}{\sqrt{2m\omega}}$ and $\hat{p} = \frac{i\sqrt{2m\omega}(\hat{a}^+ - \hat{a})}{2}$ in the form of creation $\hat{a}^+$ and annihilation $\hat{a}$ operators that act on the ground state with the rest mass m, and ω is the angular frequency of a particle in the quantum harmonic oscillator (QHO) model in QM, then we can describe the quantization of the Gaussian form of wavefunctions in a secondary space and extend it to QCD [18,19]. Hence, using the canonical variables presentation and potential interaction based on QFT forms by integral representations

$$\hat{\varphi}(x) = \int dk\, \hat{a}\, e^{ik\hat{x}}$$

$$\hat{\varphi}^+(x) = \int dk\, \hat{a}^+\, e^{-ik\hat{x}}$$

$$V(x) = \int \left(\frac{dk}{2\pi}\right)^n \tilde{V}(k^2) e^{\left(-\frac{k^2}{4\omega}\right)} : e^{ik\frac{(\hat{a}^+ + \hat{a})}{\sqrt{2m\omega}}}$$

$V(x)$ is the potential interactions under Wick's spacetime ordering operators principles, i.e., "**: ■ :**". Now, we consider the transformation of radial and momentum variables r, p_r of R^n space to the new axillary variable $s^{2\xi}, p_s$ of R^η . This axillary space is the secondary space under transformation

$r = s^{2\xi}, p_r \to p_s$, then the wavefunction can be transformed to $\Psi(r) \to q^{2\xi(n_\omega - 2n_r)}\Phi(s^2)$, where the secondary space has a dimension

$$\eta = 4s(n_\omega - 2n_r) + 2\xi + 2 = 4\ell\xi + 2\xi + 2$$

and $n_\omega = 0,1,2,\cdots$ is the main quantum number in the QHO method, n_r is the radial excitation number n_r, and ξ is a variational parameter, which allows us to achieve the physical features of the asymptotic behavior of the bound state. To define the mass spectrum of bound states in QFT, we use QHO and QCD by explaining bound state characteristics under the field conditions, such as $\frac{d\varepsilon(\mu_b)}{d\xi} = 0$, which is described in the next paragraph [9]. Hence, we have to define the parabolic form of canonical operators with the normal ordering method in the secondary space, and also consider that the total Hamiltonian of the pair $b - b^*$ bound states interaction does not contain the core parabolic terms in the canonical variables. These conditions are a specific and central point of the QHO method in the GBM model and lead us to calculate the oscillator frequency, ω_{n_r}, of the bound state. For the growing potential with the core parabolic and Wick-ordered correction terms, we determine the parabolic form of canonical operators in the Wick ordering method and then use it in the potential terms. Hence, in this paper, we consider only the core parabolic because the nonperturbative and spin interactions are not included in our calculation. Hence, the parabolic form of the position operator is defined with the Gemma function,

$$s^{2\tau} = \omega_{n_r}^{-\tau}\Gamma\left(\frac{\eta}{2} + \tau\right)\Gamma^{-1}\left(\frac{\eta}{2}\right)$$

and the momentum operator is defined as follows

$$p_s^{2\tau} = \omega_{n_r}^{\tau}\Gamma\left(\frac{\eta}{2} + \tau\right)\Gamma^{-1}\left(\frac{\eta}{2}\right)$$

where $\tau = 1,2,3,...$, the notation and canonical operators satisfy the commutator form $[\hat{s}, \hat{p}_s] = i\hbar$, $[\hat{a}, \hat{a}^+] = \eta$. The radial Laplacian operator of RRSE in the secondary space R^η:

$$\left(H_{rel} - E(\mu_b)\right)\Psi(r) = 0$$

under transformation $r = s^{2\xi}$ reads as:

$$\frac{d^2}{dr^2} + \frac{n-1}{r}\frac{d}{dr} \;\to\; \frac{d^2}{ds^2} + \frac{\eta-1}{s}\frac{d}{ds}$$

and then RRSE of $b - b^*$ bound states within HCP interaction present as follows:

$$\left\{\frac{p_s^2}{2} + V\left(s^{2\xi}\right) - E(\mu_b)\right\}\Phi(q^2) = 0 \tag{9}$$

As we know, the spin Hamiltonian is highly significant. However, the primary focus of this article is on defining the relativistic effects of bound states using the GBM and QHO methods. Therefore, in the supplementary calculations, the spin Hamiltonian $H_s = H_{SS} + H_{LT} + H_{TT}$ has not been incorporated, and its additional effects on the mass spectrum have been ignored. Now, using the parabolic form of canonical operators, Eq. (9), RRSE for the excited radial states in secondary space under the second quantization within $V(r) = -V_0\frac{e^{\alpha r} - e^{-\alpha r}}{e^{\alpha r} + e^{-\alpha r}} + \sigma r$, HCP is defined in the following way [9].

$$\varepsilon(\mu_b) = \left\{\frac{\eta\omega_\ell}{4} + 2\mu_b\xi^2 s^{4\xi-2}\left(-V_0\frac{e^{\left(\alpha s^{2\xi}\right)} - e^{-\left(\alpha s^{2\xi}\right)}}{e^{\alpha\left(\alpha s^{2\xi}\right)} + e^{-\alpha\left(\alpha s^{2\xi}\right)}} + \sigma s^{2\xi}\right) - 2\mu_b\xi^2 s^{4\xi-2}E(\mu_b) + n_\omega\omega_\ell\right\}\Phi(q^2) = 0 \tag{10}$$

The ground state $n_\omega = n_r = 0$, mass spectrum by expanding HCP under the Bernoulli series and the parabolic form of the position operator $s^{2\tau}$, and using (7) gives us [20,21].

$$M = \left(4m_b^2 - 2\mu_b^2\frac{dE(\mu_b)}{d\mu_b}\right)^{1/2} + \frac{\mu_b}{2}\frac{dE(\mu_b)}{d\mu_b} + +E(\mu_b) \tag{11}$$

where the ground state energy eigenvalue reads as

$$E_0(\mu_b) = \frac{\omega_0^{2\xi}\Gamma^{-1}\left(\frac{\eta}{2}+2\xi+1\right)\Gamma\left(\frac{\eta}{2}+1\right)}{8\mu_b\xi^2} + \frac{(\sigma-\alpha V_0)\Gamma^{-1}\left(\frac{\eta}{2}+2\xi+1\right)\Gamma\left(\frac{\eta}{2}+3\xi+1\right)}{\omega_0^{\xi}} + \frac{(\alpha^3 V_0)\Gamma^{-1}\left(\frac{\eta}{2}+2\xi+1\right)\Gamma\left(\frac{\eta}{2}+5\xi+1\right)}{3\omega_0^{3\xi}} \tag{12}$$

Then, minimizing $\frac{d\varepsilon(\mu_b)}{d\xi} = 0$ and $\frac{d\varepsilon(\mu_b)}{d\omega} = 0$, the ground state oscillator frequency ω_0 and the energy eigenvalue function is defined using the relation

$$\frac{dE(\mu_b)}{d\mu_b} = -\frac{\omega_0^{2\xi}\Gamma^{-1}\left(\frac{\eta}{2}+2\xi+1\right)\Gamma\left(\frac{\eta}{2}+1\right)}{8\mu_b^2\xi^2}$$

in the above equations, and the oscillator frequency ω_0 is defined as follows.

$${\omega_0}^{5\xi} - \frac{4(\sigma-\alpha V_0)\mu_b\xi^2\Gamma\left(\frac{\eta}{2}+3\xi+1\right)}{\Gamma\left(\frac{\eta}{2}+1\right)}{\omega_0}^{2\xi} - \frac{4(\alpha^3 V_0)\mu_b\xi^2\Gamma\left(\frac{\eta}{2}+5\xi+1\right)}{\Gamma\left(\frac{\eta}{2}+1\right)} = 0 \tag{13}$$

and the constituent mass as a relativistic effect on mass in the vacuum state μ_b reads as

$$\mu_b = \left(m_b^2 + \frac{\Gamma(\frac{\eta}{2}+1)\omega_0^{2\xi}}{16\xi^2\Gamma(\frac{\eta}{2}+2\xi+1)} \right)^{1/2} \tag{14}$$

Now, based on Eqs. (10) and (12), we can define the mass spectrum, energy eigenvalue, and oscillator frequency in the highly radial resonance states $n_r = \frac{n_\omega - \ell}{2}$ by the following equations [22].

$$E_{n_r}(\mu_b) = (\frac{1}{8} + \frac{n_r}{\eta}) \frac{\Gamma(\frac{\eta}{2}+1)}{\mu_b \xi^2 \Gamma(\frac{\eta}{2}+2\xi+1)} \omega_{n_r}^{2\xi} + \frac{(\sigma - \alpha V_0)\Gamma(\frac{\eta}{2}+3\xi+1)}{\Gamma(\frac{\eta}{2}+2\xi+1)\omega_{n_r}^{\xi}} + \frac{(\alpha^3 V_0)\,\Gamma\left(\frac{\eta}{2}+5\xi+1\right)}{3\Gamma(\frac{\eta}{2}+2\xi+1)\omega_{n_r}^{3\xi}} \tag{15}$$

$$\frac{(\sigma - \alpha V_0)\mu_b \xi^2 \Gamma\left(\frac{\eta}{2}+3\xi+1\right)}{(\frac{1}{8}+\frac{n_r}{\eta})\Gamma\left(\frac{\eta}{2}+1\right)} {\omega_{n_r}}^{2\xi} - \frac{(\alpha^3 V_0)\mu_b \xi^2 \Gamma\left(\frac{\eta}{2}+5\xi+1\right)}{4(\frac{1}{8}+\frac{n_r}{\eta})\Gamma\left(\frac{\eta}{2}+1\right)} = 0 \tag{16}$$

The constituent mass μ_b of the highly bound states reads as

$$\mu_b = \left(m_b^2 + 2(\frac{1}{8} + \frac{n_r}{\eta}) \frac{\Gamma(\frac{\eta}{2}+1)\omega_{n_r}^{2\xi}}{\xi^2 \Gamma(\frac{\eta}{2}+2\xi+1)} \right)^{1/2} \tag{17}$$

We now calculate the mass spectra of Bottomia using the non-relativistic Eq. (1) and relativistic Eq. (2) equations [11]. The results of Bottomia bound states in the QHO and GBM models are presented using specific parameters [23] in Table 1.

$$m_b = m_{b^*} = 4.823 GeV$$

$$V_0 = 1.1 GeV, \quad \alpha = 0.1 GeV$$

$$\sigma = 0.25 GeV^2$$

We chose parameters to adjust the calculation of the mass spectrum based on theoretical data from other sources and experimental results. However, these parameters are defined only at the extreme point of bound state formation and are not adjusted in this calculation for the long-range stability of bound states. We also considered $a = \sigma - V_0\alpha > 0, \quad a \neq 0$, $V_0 \neq 0$, which are extreme values solely for the creation of bound states, especially for highly resonant states. Hence, we can use experimental data and compare these values. Despite the predicted heavy mass of $b - b^*$in the highly radial excitation $n_r = 7, 8, 9, 10$ states, such as $7s: \Upsilon(10860)$ and $10s: \Upsilon(11020)$, the relativistic effects become more apparent, leading to significant internal motion and increasing the relativistic behavior of $b - b^*$ bound state. We defined quantitative error analysis using the Root Mean Square Error (RMSE), which measures the difference between the relativistic and non-relativistic values based on our approach to calculating the masses of bound states, and compared these values with experimental data. All values in our calculations are in *GeV*.

In this paper, we investigate this effect on the mass spectra and describe how it affects the shape of the potential interaction. In this article, we include only the kinetic and mass-dependent terms, as well as the effective potential related to the relativistic mass correction, in our calculation. The effective potential that is described in this research under the QHO and GBM models is based on the Schrödinger equation.

$$\left(\frac{-1}{2\mu_b}\left(\frac{d^2}{dr^2} + \frac{n-1}{r}\frac{d}{dr}\right) + \frac{\ell(\ell+1)}{2\mu r^2} - V_0 \frac{e^{\alpha r} - e^{-\alpha r}}{e^{\alpha r} + e^{-\alpha r}} + \sigma r\right)\Psi(r) = E(\mu_b)\Psi(r) \rightarrow$$

$$\left\{\frac{p_s^2}{2} + 2\mu_b \xi^2 s^{4\xi-2}\left(-V_0 \frac{e^{(\alpha s^{2\xi})} - e^{-(\alpha s^{2\xi})}}{e^{\alpha(\alpha s^{2\xi})} + e^{-\alpha(\alpha s^{2\xi})}} + \sigma s^{2\xi}\right)\right\}\Phi(q^2) = E(\mu_b)\Phi(q^2)$$

determines as follows:

$$V_{eff}(s) = 2\mu_b \xi^2 s^{4\xi-2}\left(-V_0 \frac{e^{(\alpha s^{2\xi})} - e^{-(\alpha s^{2\xi})}}{e^{(\alpha s^{2\xi})} + e^{-(\alpha s^{2\xi})}} + \sigma s^{2\xi}\right) \tag{18}$$

and presents a short-range attractive term and a long-range confinement term, including the effect of ℓ - the angular momentum quantum number, which appears in the given parameters μ_b, ξ in the following form

Table 1. Comparison of the mass spectrum in the lower and higher states of bottomia

	M_{nonrel}	M_{rel}	μ_b	M_{Th}	M_{Exp}	RMSE *Nonrel*	RMSE *Rel*
$\mathbf{1s}: \Upsilon(\mathbf{94603})$	9.2692	9.4582	4.8390	9.463 [25-27]	9.4603 [11]	0.1913	0.0021
$\mathbf{2s}: \Upsilon(\mathbf{10023})$	10.2354	10.3068	4.9048	10.023[23, 28]	10.023 [24]	0.2125	0.2840
$\mathbf{7s}: \Upsilon(\mathbf{10860})$	10.6709	10.8424	5.0039	10.887 [23]	10.885 [24]	0.2144	0.0421
$\mathbf{10s}: \Upsilon(\mathbf{11020})$	10.8296	11.0522	5.0513	11.021 [23]	11.020 [24]	0.1904	0.0322

$$\mu_b = \left(m_b^2 + 2\left(\frac{1}{8} + \frac{n_r}{4\ell\xi+2\xi+2}\right) \frac{\Gamma\left(\frac{4\ell\xi+2\xi+2}{2}+1\right)\omega_{n_r}^{2\xi}}{\xi^2\Gamma\left(\frac{4\ell\xi+2\xi+2}{2}+2\xi+1\right)} \right)^{1/2} \quad (19)$$

$$\frac{d}{d\xi}\left[\left(\frac{1}{8} + \frac{n_r}{4\ell\xi+2\xi+2}\right) \frac{\Gamma\left(\frac{4\ell\xi+2\xi+2}{2}+1\right)}{\mu_b\xi^2\Gamma\left(\frac{\eta 4\ell\xi+2\xi+2}{2}+2\xi+1\right)} \omega_{n_r}^{2\xi} + \right.$$

$$\left. \frac{(\sigma-\alpha V_0)\Gamma\left(\frac{4\ell\xi+2\xi+2}{2}+3\xi+1\right)}{\Gamma\left(\frac{4\ell\xi+2\xi+2}{2}+2\xi+1\right)\omega_{n_r}^{\xi}} + \frac{(\alpha^3 V_0)\,\Gamma\left(\frac{4\ell\xi+2\xi+2}{2}+5\xi+1\right)}{3\Gamma\left(\frac{4\ell\xi+2\xi+2}{2}+2\xi+1\right)\omega_{n_r}^{3\xi}} \right] = 0 \quad (20)$$

To plot the shape of the effective potential based on the non-RRSE and RRSE, we used the relativistic and non-relativistic mass spectra and the constituent mass of quarks in $1s{:}\,\Upsilon(94603)$ in the ground state $n = 0, \ell = 0, n_r = 0$, $2s{:}\,\Upsilon(10023)$ in the first excited state, and two predicted highly excited states $7s{:}\,\Upsilon(10860)$ and $10s{:}\,\Upsilon(11020)$. The results of shape, depth, and asymptotic lines of potential are affected by changing the reduced mass of the $b-b^*$ bound state. From the curve and shape of the effective potential function, we can determine the minimum point where and how steep the transition occurs, and potential wall behaviors provide the properties of the bound state. As we can see in the relativistic and non-relativistic plots in Figs. 1 and 2, the mass of the bound state changes the curvature of the curve of the potential shape. In the highly bound state mass value (highly resonance states), the shape becomes deeper, which allows us to determine the minimum energy eigenvalue in the mass spectra of the bound states. These properties can help us understand the internal dynamics of bound states.

In high energy physics, the properties of potential interactions are an interesting open question for future research at the LHC, the Super KEKB accelerator (Belle II), the ALICE Experiment, the LHCb Experiment, CMS, and ATLAS. Therefore, by plotting HCP with different potential parameters, we can explain the sensitivity of mass spectra and the shape of potential in QHO and GBM models, and analyze the experimental data. The form of the plot and the depth of the potential well can be used to assign the other hadronic states to be constituted of more than two quarks. Based on the QHO and GBM models, one can obtain a suitable HCP to explain the dynamics of the hadronic bound states by applying relativistic corrections to the mass without involving spin interactions. 3D HCP shapes and mass spectra based on non-RRSE and RRSE can represent how sensitive the depth of the potential well is to the relativistic mass correction. The results of the relativistic correction on the effective potential of Bottomia bound states were performed using MATLAB R2021a software and Excel 2022, and are presented in Figs. 1 and 2.

4. Conclusion

This study concentrates on describing the asymptotic behavior of the polarization loop function in the quantum gauge interaction to define the mass spectrum of bound Bottomia states, taking into account the relativistic correction to the mass of constituent particles in high energy physics. Comparing non-relativistic mass spectra and relativistic correction on mass spectra based on the modified Schrödinger equation, we can conclude that our results may explain and predict resonance states using the 3D HCP well's shape of the pair $b-b^*$ bound states. Based on the results presented in Table 1, as defined analytically using QHO and GBM models, we can summarize the main concepts as follows:

1- The modified Schrödinger equation under the relativistic correction on mass is investigated by applying the QHO and GBM models.

2- The exponential and linear confinement type of potential is used to determine the mass spectra of Bottomia $1s{:}\,\Upsilon(94603)$, $2s{:}\,\Upsilon(10023)$, $7s{:}\,\Upsilon(10860)$, and $10s{:}\,\Upsilon(11020)$.

3- The analytical expression of the constituent mass μ_b and reduced mass $\mu = \frac{\mu_b}{2}$ are presented. Results are used to describe mass spectra under both relativistic and non-relativistic formalisms.

4- Defined numerical results are compared with the experimentally well-established low-level states $1s{:}\,\Upsilon(94603), 2s{:}\,\Upsilon(10023)$ and high resonance states $7s{:}\,\Upsilon(10860)$, and $10s{:}\,\Upsilon(11020)$. For these S-wave states, our calculation has percent differences, computed as

	$\Delta M\%$
$\mathbf{1s{:}\,\Upsilon(94603)}$	-0.02
$\mathbf{2s{:}\,\Upsilon(10023)}$	+2.83
$\mathbf{7s{:}\,\Upsilon(10860)}$	-0.39
$\mathbf{10s{:}\,\Upsilon(11020)}$	+0.29

In the first excited state, our value is approximately 2.83 % larger than the experimental one; the reason for this difference can be found in the total Hamiltonian of interactions. In the Bottomia Hamiltonian of hyperfine (triplet and singlet levels), spin–orbit and tensor interactions are important. Conversely, the nonperturbed Hamiltonian term, which includes the relativistic behavior of potential interaction and high-temperature conditions, can shift the mass spectra to some disagreement with experimental data.

5- We used purely static potential, no perturbative loop corrections, and no higher-order momentum-dependent terms $p_s^{2\tau}$ with $\tau = 2{,}4$; hence, these terms can justify some disagreement between our results and the experimental data.

Therefore, as we know, the first radial excited state feels the short-distance Coulombic potential more than the ground state. Since we did not directly include αs as a coupling constant, it makes the first radial existing state mass spectrum $+2.83$ % too heavy.

6- Using the boundary condition of potential depth V_0, theoretically calculated and predicted by applying the QHO and GBM models, as well as other higher resonance states, such as $11s$ and $12s$. With the relativistic bound state masses 11.1148, 11.1748, and non-relativistic 10.8758, 10.9195, the constituent mass of the bottom quark 5.0662 and 5.0809 are determined in $11s$ and $12s$ states, which have not yet been discovered or confirmed [29,30].

The QHO and GBM methods employed in this theoretical research are among the most established approaches in the calculation and prediction of hadronic bound states.

Therefore, theoretical calculations with optimized and modified potentials for the structure of the strong interaction can provide new and different approaches, especially from a particle physics perspective, as accelerator and LHC technologies continue to evolve and improve. One of these approaches is discussed in this article. This approach describes the behavior and properties of the bound Bottomia within the relativistic mass correction.

Acknowledgment

The author would like to acknowledge the use of AIA and tools to improve the grammar and clarity of this manuscript. All intellectual content and conclusions are solely those of the author. We are indebted to the referees and are very grateful for their careful reading, comments, and detailed suggestions, which helped us to improve the manuscript considerably.

Funding

The theoretical research described here was supported by Buein Zahra Technical University grant (number 1404).

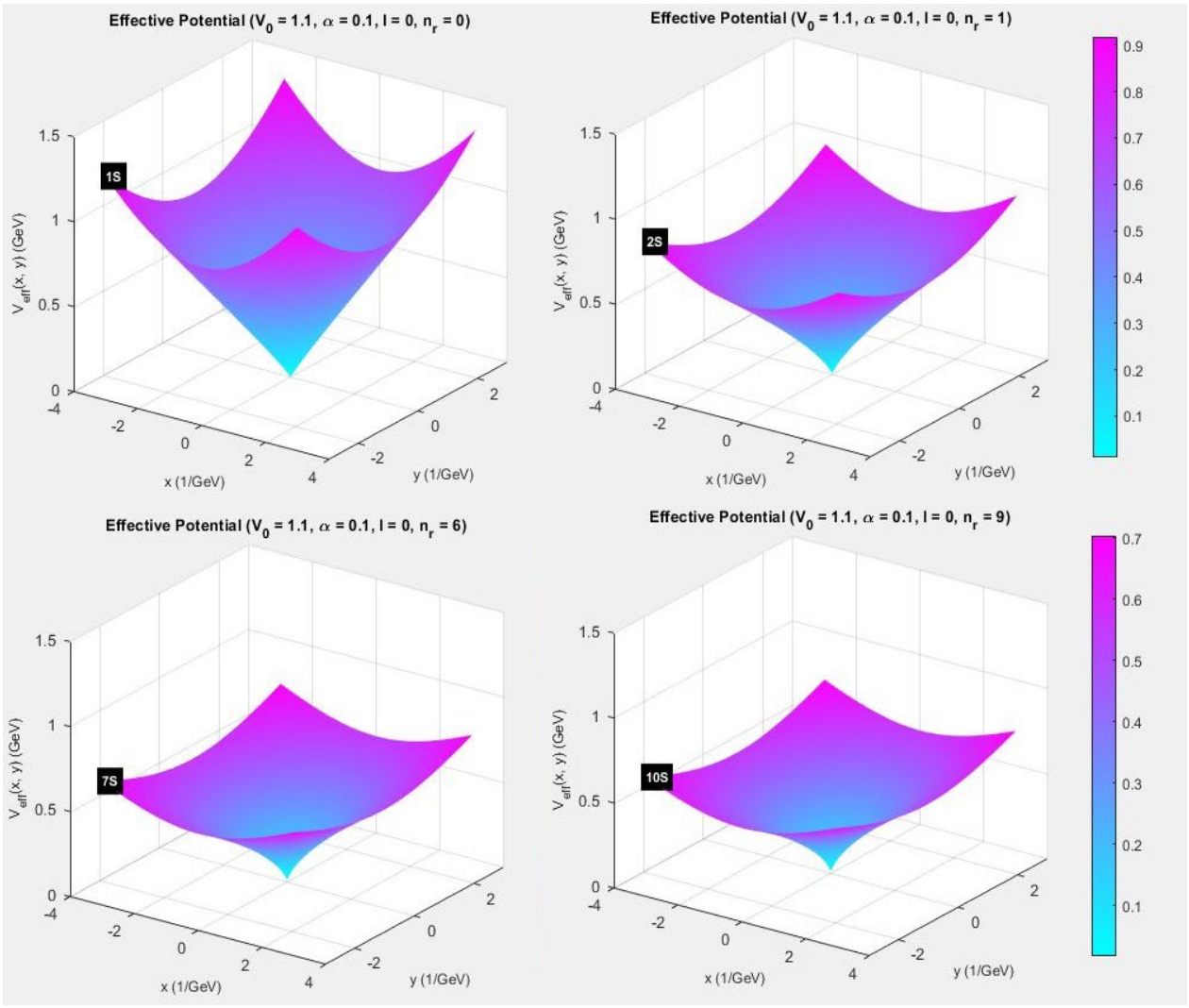

Fig. 1. Effective potential well with the relativistic correction on mass.
Note. $1s$: $\Upsilon(94603)$, $2s$: $\Upsilon(10023)$, $7s$: $\Upsilon(10860)$, $10s$: $\Upsilon(11020)$.

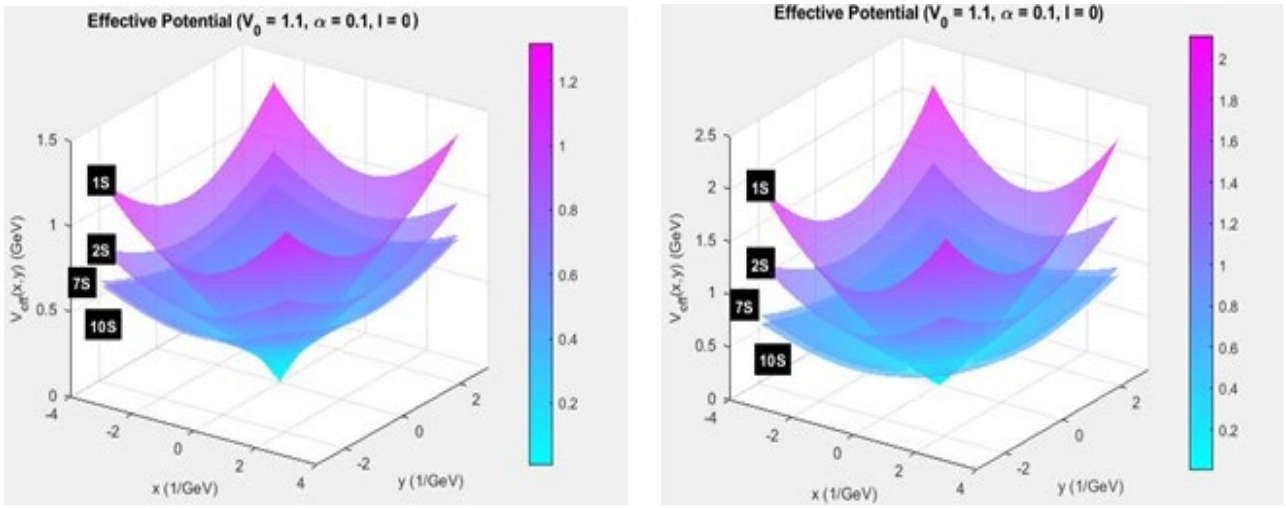

Fig. 2. Multiple surfaces of the effective potentials: left (RRSE) and right (non-RRSE).
Note. $1s$: $\Upsilon(94603)$, $2s$: $\Upsilon(10023)$, 7s: $\Upsilon(10860)$, 10s: $\Upsilon(11020)$.

Disclosure statement

No potential conflict of interest was reported by the authors.

References

[1] Yoh, J. (1998). The Discovery of the b Qquark at Fermilab in 1977: The Experiment Coordinator's Story. *AIP Conference Proceedinds, 424*(1), 29-42. https://doi.org/10.1063/1.55114

[2] Asner, D. M., Atmacan, H., Banerjee, Sw., Bennett, J. V., Bertemes, M., & Bessner, M. *et al.* (2022). Belle II Executive Summary, *arXiv:2203.10203v2*[hep-ex]. https://doi.org/10.48550/arXiv.2203.10203

[3] Brambilla, N., Eidelman, S., Hanhart, C., Nefediev, A., Shen, C., & Thomas, C. E. *et al.* (2020). The xyz States: Experimental and Theoretical Status and Perspectives, *Physics Reports, 873*, 1-154. https://doi.org/10.1016/j.physrep.2020.05.001

[4] Bokade, C. A., & Bhaghyesh (2025). Predictions for Bottomonium from a Relativistic Screened Potential Model, *arXiv: 2501.03147v1*[hep-ph]. https://arxiv.org/pdf/2501.03147v1

[5] Tang, Z., Wu, B., Hanlon, A., Mukherjee, S., Petreczky, P., & Rapp, R. (2025). Quarkonium Spectroscopy in the Quark-Gluon Plasma, *arXiv:2502.09044v1*[nucl-th]. https://doi.org/10.48550/arXiv.2502.09044

[6] Fujiwara, D. (2017). *Rigorous Time Slicing Approach to Feynman Path Integrals* (1st ed.). Springer. https://doi.org/10.1007/978-4-431-56553-6

[7] Struckmeier, J. (2024). Relativistic Generalization of Feynman's Path Integral Based on Extended Lagrangians. *arXiv:2406.06530v1*[quant-ph]. https://doi.org/10.48550/arXiv.2406.06530

[8] Semenoff, G. W. (2023). *Quantum Field Theory: An Introduction* (1st ed.). Springer Singapore. https://doi.org/10.1007/978-981-99-5410-0

[9] Dienykhan, M., Efimov, G. V., Ganbold, G., & Nedelko, S. N. (1995). *Oscillator Representation in Quantum Physics*. In Lecture Notes in Physics Monographs (1st ed.). Springer Berlin. https://doi.org/10.1007/978-3-540-49186-6

[10] Greiner, W., Schramm, S., & Steinm W. (2007). *Quantum Chromodynamics* (3rd ed.). Springer Berlin. https://doi.org/10.1007/978-3-540-48535-3

[11] Gould, R., (2020). *Quantum Electrodynamics. Electromagnetic Processes* (1st ed.). Springer-Verleg.

[12] Albeverio, S., Høegh-Krohn, R., & Mazzucchi, S. (2008). *Mathematical Theory of Feynman Path Integrals: An Introduction* (1st ed.). Springer Berlin. https://doi.org/10.1007/978-3-540-76956-9

[13] Copson, E. T. (2009). *Asymptotic Expansions: The Saddle-Point Method* (1st ed.). Cambridge University Press. https://doi.org/10.1017/CBO9780511526121

[14] Barley, K., Vega-Guzm, J., Ruffing, A., & Suslov, S. K. (2022). Discovery of the Relativistic Schrödinger Equation. *Journal of Experimental and Theoretical Physics, Russian Academy of Sciences, 65*(1), 90-103. https://doi.org/10.3367/ufne.2021.06.039000

[15] Badalov, V., & Badalov, S. (2023). Generalised Tanh-Shaped Hyperbolic Potential: Klein–Gordon Equation's Bound State Solution. *Communications in Theoretical Physics, 75*(7), 075003. https://doi.org/10.1088/1572-9494/acd441

[16] Kher, V., Chaturvedi, R., Devlani, N., & Rai, A. K. (2022). Bottomonium Spectroscopy Using Coulomb Plus Linear (Cornell) Potential. *The European*

Physical Journal Plus, 137, 357. https://doi.org/10.1140/epjp/s13360-022-02538-5

[17] Kutzelnigg, W. (1994). Theory of the Expansion of Wave Functions in a Gaussian Basis. *Quantum Chemistry Journal, 51*(6), 447-463. https://doi.org/10.1002/qua.560510612

[18] Rushka, M., & Freericks, J. K. (2019). A Completely Algebraic Solution of the Simple Harmonic Oscillator. *American Journal of Physics, 88*(11), 976-985. https://doi.org/10.1119/10.0001702

[19] Kelley, J. D., & Leventhal, J. J. (2017). Ladder Operators for the Harmonic Oscillator. In *Problems in Classical and Quantum Mechanics*. Springer. https://doi.org/10.1007/978-3-319-46664-4_7

[20] Lehmer, D. H. (1940). On the Maxima and Minima of Bernoulli Polynomials. *American Mathematical Monthly, 47*(8), 533-538. https://doi.org/10.2307/2303833

[21] Sun, Z.-W., & Pan, H. (2006). Identities Concerning Bernoulli and Euler Polynomials. *Acta Arithmetica. 125*(1), 21-39. http://eudml.org/doc/278468

[22] Shafie, A., Naji, J., Jahanshir, A., & Heshmatian, S. (2023). Approximation and Analytical Study of the Relativistic Confined Two Particles State within the Complex Potential in the Isotropic Medium. *Journal of Particle Science and Technology, 9*(2), 85-101. https://doi.org/10.22104/jpst.2024.6528.1243

[23] Ahmadov, A. I., Abasova, K. H., Orucova, M. Sh. (2021). Bound State Solution Schrödinger Equation for Extended Cornell Potential at Finite Temperature. *Advances in High Energy Physics, 2021*, 1861946. https://doi.org/10.1155/2021/1861946

[24] Particle Data Group (2020). Review of Particle Physics. *Progress of Theoretical and Experimental Physics, 2020*(8), 083C01. https://doi.org/10.1093/ptep/ptaa104

[25] Badalov, V., Ahmadov, A. I., Dadashov, E. A., & Badalov, S. V.. (2025). Dirac Equation Solution with Generalized Tanh-Shaped Hyperbolic Potential: Application to Charmonium and Bottomonium Mass Spectra. *arXiv:2409.15538v3*[hep-ph]. https://doi.org/10.48550/arXiv.2409.15538

[26] Abu-Shady, M. (2016). Heavy Quarkonia and bc* Mesons in the Cornell Potential with Harmonic Oscillator Potential in the N-Dimensional. *International Journal of Applied Mathematics and Theoretical Physics, 2*(2), 16-20. https://doi.org/10.11648/j.ijamtp.20160202.11

[27] Bukor, B., & Tekel, J. (2023). On Quarkonium Masses in 3D Non-Commutative Space. *The European Physical Journal Plus, 138*, 499. https://doi.org/10.1140/epjp/s13360-023-04049-3

[28] Purohit, K. R., Jakhad, P., & Rai, A. K. (2022). Quarkonium Spectroscopy of the Linear Plus Modified Yukawa Potential. *Physica Scripta, 97*(4), 044002. https://doi.org/10.1088/1402-4896/ac5bc2

[29] Li, Q., Liu, M.-S., Lü, Q.-F., Gui, L. C. & Zhong, X.-H.(2020). Canonical Interpretation of *Y*(10750) and ϒ(10860) in the ϒ Family. *The European Physical Journal C, 80*(1), 59. https://doi.org/10.1140/epjc/s10052-020-7626-2

[30] Wang, J., & Liu, X. (2024). Identifying a Characterized Energy Level Structure of Highly Charmonium Well Matched to the Peak Structures in $e^+e^- \to \pi^+ D^0D^{*-}$. *Physics Letters B, 849*(8), 138456. https://doi.org/10.1016/j.physletb.2024.138456

Additional information

Correspondence and requests for materials should be addressed to A. Jahanshir.

HOW TO CITE THIS ARTICLE

Jahanshir, A.; Omugbe, E. (2025). Effects of hybrid confinement potential on predictable hadronic highly resonance states*, J. Part. Sci. Technol. 11(1) 1-10.*

DOI: 10.22104/jpst.2025.7612.1277
URL: https://jpst.irost.ir/article_1559.html